Prevention of cartilage dehydration in imaging studies with a customized humidity chamber

Ryan J. Choo, Colin Firminger, Ralph Müller, and Kathryn S. Stok
Institute for Biomechanics, ETH Zurich, Zurich 8093, Switzerland

(Received 9 April 2013; accepted 25 August 2013; published online 12 September 2013)

Quantitative three-dimensional imaging methods such as micro-computed tomography (μCT) allow for the rapid and comprehensive evaluation of cartilage and bone in animal models, which can be used for drug development and related research in arthritis. However, when imaging fresh cartilage tissue in air, a common problem is tissue dehydration which causes movement artifact in the resulting images. These artifacts distort scans and can render them unusable, leading to a considerable loss of time and effort with sample preparation and measurement. The sample itself is also irretrievably damaged by the dehydration, often unable to return to its full tissue thickness upon rehydration. Additionally, imaging with ionic contrast agents such as Hexabrix™ must be performed in air, otherwise the agent will be washed out if immersed in a liquid. The first goal of this study was to design a customized humidity chamber to maintain cartilage hydration without the need for immersion. Following this, the use of the humidity chamber during a synchrotron radiation-μCT scan was validated and its performance evaluated. Results showed that the loss of fluid film volume is associated with scanning at low humidity (87%), and can be avoided using the humidity chamber. Coupling this technology with advances in synchrotron imaging (e.g., phase contrast imaging) or contrast agents is promising.
 [http://dx.doi.org/10.1063/1.4820913]

I. INTRODUCTION

Arthritis is a painful and slow-developing chronic disease that involves the degradation of articular cartilage and affects millions of people worldwide. It is characterized by architectural and structural alterations to the cartilage and underlying bone matrices, chemical and molecular changes to their composition, and modifications to the mechanics of the functional joint. Changes to bulk tissue morphometry and their effect on individual components, as well as the spatially varying relationships (from the surface to the deep zones) between the structures in the cartilage and how they interact, have been proposed as aspects demanding more detailed characterization for understanding arthritis. In turn, there is a need for imaging tools allowing reproducible quantification of cartilage for provision of high-resolution quantitative 3D data sets and for accurate correlation between mechanical and biological signaling pathways.

In order to image soft tissues such as cartilage, ligaments, and tendons, imaging modalities need to account for their water content. This is especially the case for cartilage, whose water content accounts for up to 84% of its wet weight[1] and is vitally important to its mechanical and physiological properties. For smaller samples, the rate of water loss by evaporation can be extremely quick. This evaporation is influenced by atmospheric humidity and ambient temperature[2] and can cause tissue shrinkage. However, it is imperative that soft tissue samples used for physical tests remain fully hydrated. In this work, a device was developed to support cartilage imaging and maintain sample hydration during scanning.

Quantitative three-dimensional (3D) imaging methods such as microcomputed tomography (μCT) and synchrotron radiation-microcomputed tomography (SR-μCT) allow for the rapid and comprehensive evaluation of cartilage and bone in animal models, and can be used for drug development[3] and related research in arthritis.[4] μCT alone is not useful for the direct imaging of soft tissue structures and biochemistry due to the low X-ray absorption of the non-mineralized extracellular matrix components. However, when used in conjunction with a radiographic and ionic contrast agent, cartilage tissues can be visualized. This technique is called equilibrium partitioning of an ionic contrast agent via μCT, EPIC-μCT.[5]

EPIC-μCT exploits the electrochemical interactions between the negatively charged glycosaminoglycan (GAG) content found in cartilage with an ionic contrast agent.[5] Hexabrix™ is a clinically available CT contrast agent containing a negatively charged ioxaglate ion that is typically used for this type of imaging. When cartilage is immersed in Hexabrix prior to scanning, the negatively charged ioxaglate ions repel the negatively charged content in cartilage. The equilibrium distribution of the contrast agent is non-uniform and has been shown to be inversely proportional to GAG density.[5,6] Other contrast agents can provide similar results.[7] In anionic-contrast-enhanced μCT images, regions with low X-ray attenuation are indicative of higher GAG density, while areas with high X-ray attenuation correspond to lower GAG density. In this way, grayscale values can be used to obtain quantitative measures of cartilage GAG composition and also tissue morphometry.

Other imaging modalities such as scanning electron microscopy (SEM) can achieve resolutions visualizing individual collagen fibrils in the cartilage matrix.[8] However, it also requires specimens to be completely dry since they are scanned under high vacuum,[2] or it involves sample fixation (formaldehyde or cryofixation) leading to sample fracture and damage during preparation.[8] In fact, most other methods

available require some sample manipulation, fixation, or destruction, rather than direct imaging of the structures.[9,10]

Synchrotron radiation can offer several advantages to absorption contrast imaging because of its high intensity,[11] which allows small samples to be studied with high spatial resolution in reasonable sampling times.[12] In a study to determine collagen fibril orientations in small areas of articular cartilage using X-ray diffraction, the exposure time of several days to obtain a single X-ray diffraction pattern was reduced to 10 min using the more intense synchrotron radiation.[13] It allows quantification of the GAG content in cartilage, and the spatial resolution of SR-μCT on a submicrometer level can uncover structures of interest.[14]

However, when imaging fresh cartilage tissue in air using SR-μCT, the problem of tissue dehydration returns, which causes movement artifact in the resulting images (Figure 1). This is especially noticeable at high resolutions (6 μm and higher) and occurs even in "fast" scans of 5 min or less. Movement artifact makes it difficult to isolate structures of interest, and in severe cases, can cause the images to be rendered unusable for analysis; see Figure 1. This is problematic because significant amounts of time can be invested in sample preparation and scanning only to be lost with poor image quality. Since tissue dehydration is responsible for causing movement artifact, a device that can maintain cartilage hydration will help to counteract this problem and maintain sample integrity. Additionally, with such a device and the use of an ionic radiographic contrast agent, e.g., Hexabrix,[1] the specimens can be scanned in air, avoiding washout of the staining agent.

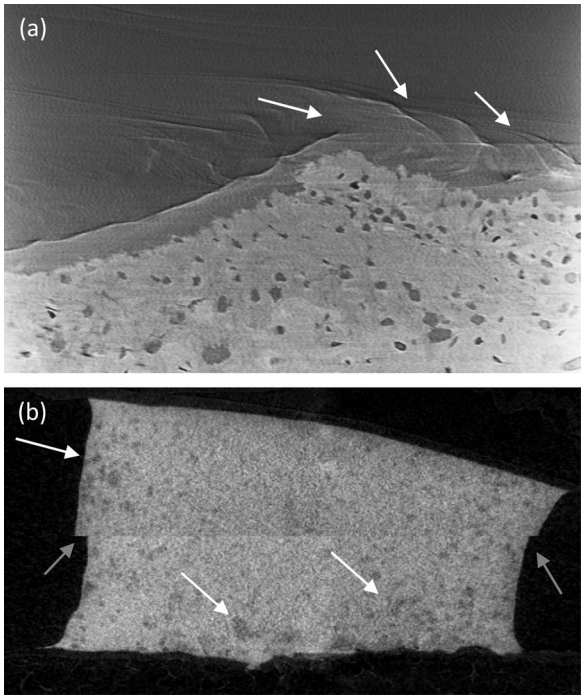

FIG. 1. (a) Motion artifact in a SR-μCT image of a mouse tibia scanned without the humidity chamber. The surface of the fluid film is not continuous. The transparent streaks in the fluid film, indicated by the white arrows, reveal movement in the scanned structure. (b) Porcine chondrocytes seeded in agarose type VII gel and cultured for 4 weeks. Samples were immersed for 30 min in 45% Hexabrix and scanned in a desktop μCT-40 (Scanco Medical, Brüttisellen-Switzerland) at 12 μm. Gray arrows indicate a stacking artifact due to dehydration of the lower half of the sample during scanning. The dark spaces indicated by the white arrows are cells in the gel structure.

Therefore, in this work, a second-generation customized humidity chamber, based on an earlier prototype,[15] was developed to preserve the relative humidity (RH%) level of specimens during scanning. A study of the humidity chamber performance was then carried out to determine: (a) whether the device could maintain sample hydration throughout a SR-μCT scan and eliminate motion artifact, and (b) whether there was a minimum relative humidity level above which cartilage dehydration could be avoided.

II. DESIGN AND ASSEMBLY OF THE HUMIDITY CHAMBER

A. Design considerations

The humidity chamber was designed for use in conjunction with the TOmographic Microscopy and Coherent rAdiology experiments (TOMCAT) beamline of the Swiss Light Source (SLS) of the Paul Scherrer Institute, and for the purpose of scanning small soft tissue samples (both *in vitro* and tissue-engineered joint tissues) at a high resolution (0.5–5.0 μm). At the time, the TOMCAT beamline was chosen because it had the desired spatial resolution for future studies. Recent advances in desktop μCT systems since then have seen improvements in spatial resolution that now rival those of the beamline.

The primary design objective of the humidity chamber project was to develop a device that could preserve the moisture content in a cartilage sample to eliminate the movement artifact associated with dehydration. This would involve raising the humidity inside the chamber to a level high enough to prevent the tissue morphometry from being altered during scanning. The device had to reach the desired humidity level in under 2 min and maintain it throughout the duration of a scan. Additionally, the ability to monitor the humidity in real time was an important design feature. In order to accommodate various sample sizes and scanning resolutions, the device needed to allow for future modularity. The size of the humidity chamber had to fit within the sample equipment regulations for the TOMCAT beamline and the entire construction had to weigh less than 2 kg to ensure compatibility with the TOMCAT stage. It was necessary for the chamber materials to be compatible with saline environments and also be radiotranslucent to avoid interference with the imaging modality. Finally, the humidity chamber had to be simple to use and require a limited amount of training. While the device was designed with cartilage in mind, it was also intended for use in tissue-engineering studies to image a variety of other materials and soft tissues.

B. Pilot work

An experimental box mimicking the conditions of the humidity chamber was built to establish the initial design parameters and serve as a proof of concept for the device. Strips of cartilage were placed in the box, mimicking various humidity conditions, and the reduction in sample length was recorded over time. The box was placed under the stereomicroscope in

order to precisely measure the change in length. The velocity of shrinkage of a cartilage sample in the box was measured over a period of 45 min in a range of temperature and humidity conditions (where temperature was controlled and humidity monitored): (i) exposed to the open air at room temperature (control), and enclosed in the box at (ii) room temperature, (iii) 33 °C, and (iv) 37 °C. A sponge moistened with water was placed at the bottom of the box to create humidity and a heater was placed underneath the box to control temperature. The velocity of shrinkage was found to be highest at the beginning of each experiment, approaching 180 μm/min for the control case and reduced to 80 μm/min when the experimental box was used (at room temperature), demonstrating the feasibility of the humidity chamber concept. The velocity of shrinkage was observed to decrease to less than 5 μm/min when the humidity was raised and maintained above 90%. This suggested that the optimal conditions for the humidity chamber were above 90%. Using temperature control to control humidity, a prototype was built and tested. Although it was able to raise the humidity in the chamber above 90%, this level could not be reliably maintained during testing. Therefore, instead of controlling the temperature, a new device was developed to set the humidity level in the chamber.

C. Assembly

The humidity chamber consists of three major components: a sample lid, a holder, and an outer tube, Figure 2(a) (a′, d′, and e′). The holder houses a heating coil and a SHT75 digital humidity sensor (Sensiron, Stäfa, CH) which is capable of measuring the temperature and RH% in the chamber, Figure 2(c) (c′ and d′). A custom firmware developed in Labview (National Instruments, Texas, USA) is used to monitor and control the temperature and RH% to ensure that the humidity is maintained at the desired level. This setup is capable of maintaining the RH% within the chamber above 92% and can keep the environment at a physiological temperature of 37 °C, if required.

To scan cartilage specimens, samples are first immersed in a contrast agent. They are then fixed to the humidity chamber lid using superglue (Figure 2(d)) and added to the radiotranslucent outer tube which is screwed into the holder. This creates a seal which prevents any moisture inside the chamber from escaping. The outer tube is coated with lead film to protect the temperature/humidity sensor from radiation (Figure 2(b) and 2(c), (e′)). The relative humidity inside the chamber is raised using a separate device that houses a nebulizer (DH-25B, Conrad Electronics SE, Hirschau, DE) to convert water into mist, and a ventilation unit that directs the water droplets directly into the measurement tube (Figure 2(e)). This process requires the sample lid to be removed and promptly replaced. At the SLS TOMCAT, the humidity chamber is positioned on an adjustable sample stage next to the detector (Figure 2(f)).

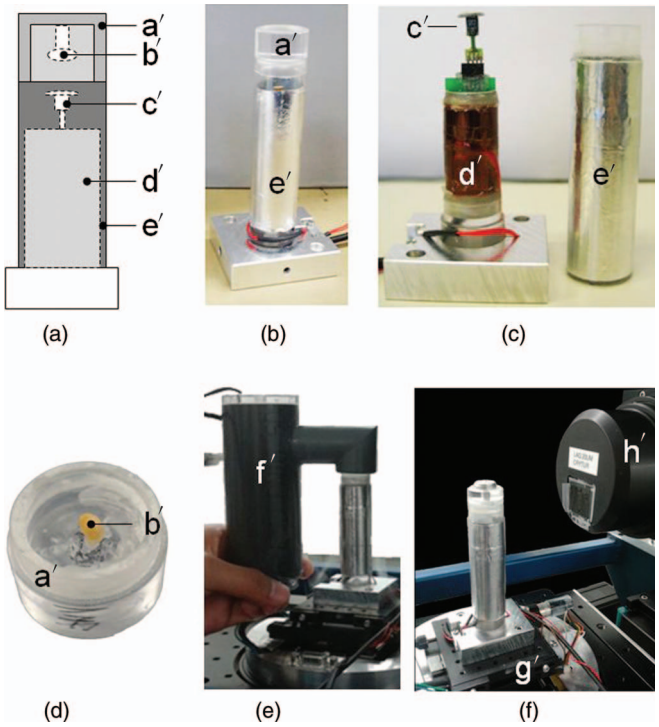

FIG. 2. (a) Concept drawing of the assembled humidity chamber; sample lid (a′) with the attached sample (b′). The humidity and temperature sensor (c′) which measures conditions inside the chamber and is protected by the outer tube (e′) from radiation. An inside holder with heater (d′) creates an air gap with the outer tube to maintain humidity. (b) The assembled chamber. (c) The chamber with the outer tube removed, and (d) the sample lid with sample attached. (e) After removing the sample lid, the nebulizer (f′) introduces water vapour in the form of mist directly into the chamber to increase relative humidity; the lid is then promptly reattached. (f) The humidity chamber positioned on the SLS TOMCAT sample stage (g′) in line with the scintillator/microscope (h′).

III. VALIDATION STUDY

A. Experimental protocol

Tibial plateaux from 6 CBA/01 mice were immersed in 40% Hexabrix (Mallinckrodt, St Louis, USA) for 2 h.[5] The samples were then placed in the humidity chamber and scanned with SR-μCT at the Swiss Light Source (Paul Scherrer Institute, Villigen, CH), using an isotropic voxel size of 3.7 μm, 4× magnification, 3.3 mm^2 field of view, and an energy of 17.5 keV. Each specimen was first placed on a sample-positioning stage in the SLS TOMCAT (Figure 2(a)). The stage is designed to allow for translational and rotational motion. The sample was then illuminated by X rays, and rotated about its longitudinal axis, perpendicular to the direction of the beam. A set of radiographs is recorded as the specimen is rotated through an angular range of 180°. The raw data that were acquired from these images was then rearranged into sinograms. These sinograms were reconstructed using filtered-backprojection to give a set of sections called tomograms. Three-dimensional visualization of the data was obtained with further processing.

This study was divided into two experiments. The tibial plateaux were scanned at decreasing RH% levels of 97%, 92%, and 87% to test for a humidity level where cartilage dehydrates and causes motion artifact. Additionally, at each RH% level, the tibial plateaux were scanned 3 times in 8 min intervals (0–8 min, 8–16 min, and 16–24 min) to test the change in cartilage volume with time due to shrinkage.

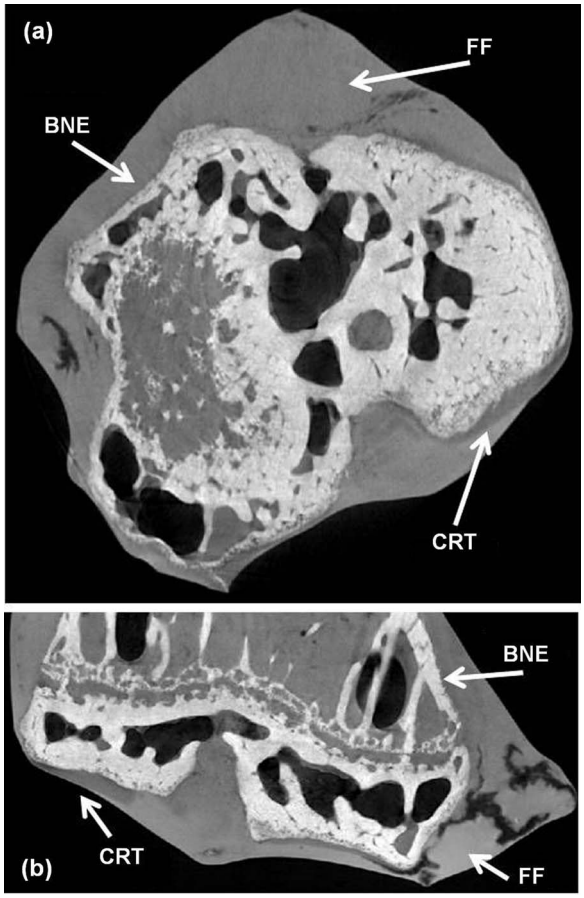

FIG. 3. Typical SR-μCT scans of a mouse tibia in the (a) axial and (b) frontal planes. Strong contrast in the image allows for the clear distinction of cartilage tissue (CRT, in dark gray) from the bone (BNE, in white) and fluid film (FF, in light gray).

B. Quantitative morphometry

During scanning, a thin fluid film covers the tibia and is a good indicator of sample hydration (Figure 3). Since the shrinkage of the film itself can induce motion artifact in the μCT images (and thus undermine the entire image quality), maintaining its hydration during a scan was vital. As such, the fluid film and cartilage tissue together were defined as the volume of interest for morphometric analysis, termed in this work as "fluid film volume." They were both treated as one structure and manually segmented from the epiphyseal region of the tibia in the SLS scans. The fluid film volume in each scan was calculated using the same methods for finding cartilage volume in previous work[14] and then plotted against time and RH%. The cartilage was also isolated (manual segmentation) from the fluid film volume to calculate the mean grayscale values in the cartilage tissue volume only at the different relative humidity levels. It was expected that as a sample dehydrates the contrast in the cartilage volume is expected to increase as the contrast agent equilibrates to a reduced (dehydrated) fluid film volume due to evaporation at the fluid film surface.

Fluid film volume was found by triangulating the surface of a voxel image and defining tetrahedrons within the structure according to the triangulated surface, where $Cg \cdot V$ is the sum of the individual tetrahedral volumes.[16] Fluid film thickness maps were determined by filling maximal spheres into the structure using distance transformation.[15,17]

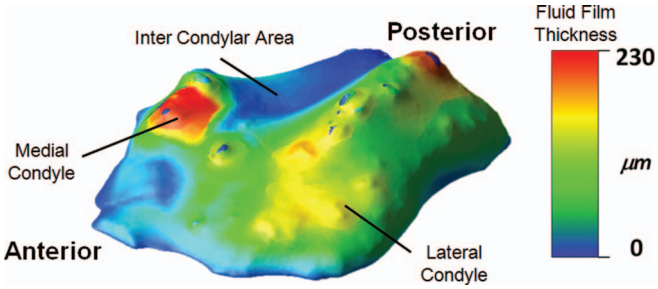

FIG. 4. A 3D thickness model of the fluid film volume that surrounds the tibia. The volume is thicker over the condyles because this area includes both the fluid film and articular cartilage.

C. Statistics

A one way analysis of variance (ANOVA) with Tukey's multiple comparison test was used to test the significance of the change in fluid film volume with the three time intervals (0–8, 8–16, and 16–24 min) and at the three relative humidity levels (87%, 92%, and 97%). A Student's one-tail, two-sample, equal variance t-test, was used to compare the fluid film shrinkage rates at 87% and 97%. For all statistics, values of $p < 0.05$ were considered significant, and $p < 0.01$ highly significant. Statistics were performed using the SPSS software package (IBM SPSS Statistics 19.0 for Windows, SPSS Inc., Chicago, USA).

IV. RESULTS

Artifact-free images of the mouse tibia that were produced at the SLS are shown in Figure 3; they exemplify the ability of the humidity chamber to maintain sample hydration during scanning. High contrast between the thin fluid film, cartilage, and bone allow them to be easily distinguished upon visual inspection. A 3D thickness map of the fluid film volume that was used for morphometric analysis is shown in Figure 4. The thicker cartilage tissue surrounding the condyles is recognizable within the fluid film.

The fluid film volume (percent of initial volume) versus time for a typical sample at 87%, 92%, and 97% relative humidity is shown in Figure 5. The loss of fluid film volume over time was observed at all humidity levels. At 87% there was a significant difference between the fluid film volumes in the 0–8 and 8–16, and between 8–16 and 16–24 min intervals. This was also seen in the 92% scans between the same intervals, but not the 97% scans, indicating that even over only 8 min scan intervals, shrinkage due to inadequate humidity levels (<97%) induces a measurable difference. Comparing the 0–8 min intervals against the 16–24 min intervals, i.e., longer scan duration, the 87% and 92% saw highly significant ($p < 0.01$) changes in fluid film volume. These changes were also observed in the 97% scans but to a lesser degree ($p > 0.05$). Although fluid film volume was lost over

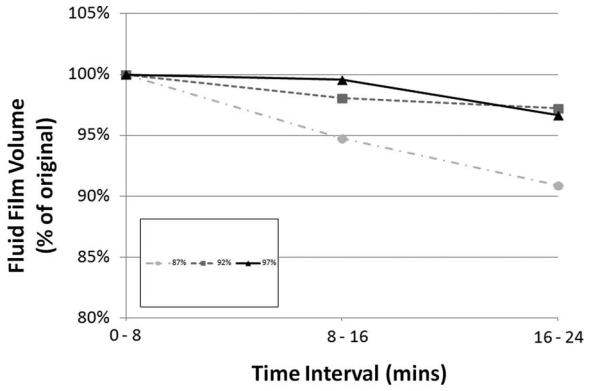

FIG. 5. Fluid film volume versus time for a typical sample at three humidity levels. The fluid film volume is more stable when scanning at higher relative humidity levels (92% and 97%). The loss of fluid film volume over time is more dramatic when scanning at low relative humidity (87%).

time during scanning with all humidity levels, this was significantly less in the 97% scans.

When comparing the normalized mean gray values of cartilage only at 87%, 92%, and 97%, as expected, an increase in cartilage contrast was observed over time; the mean gray values in the 16–24 min intervals were higher than the mean gray values in the 0–8 min intervals (i.e., increased contrast with time). The percent change in contrast was 6.0% and 6.3% for scans at 87% and 92% relative humidity, respectively, and only 3.6% at 97% (not significant (n.s.)). Additionally, when comparing the initial contrast of each humidity level (in the 0–8 min time intervals), the mean gray values measured at 87% relative humidity were larger than those at 97%. This suggests that shrinkage was already occurring during the prescan setup interval (5 min).

The gradients of fluid film volume (mm^3) versus time represent the rate of volumetric shrinkage (Table I), and are essentially an indicator of dehydration in the cartilage tissue. As expected, the rates of volumetric shrinkage for the 97% scans were relatively stable with a mean rate of -0.0023 mm^3/min (SD: 0.0017 mm^3/min), indicating that sample hydration was negligible during scanning. At 87%, the mean rate of volumetric shrinkage was -0.0047 mm^3/min (SD: 0.0019 mm^3/min), suggesting that samples were more susceptible to cartilage dehydration at this humidity. The Student's t-test shows that the volumetric shrinkage rates of both the 87% and 92% measurements were significantly greater than for the 97% measurements illustrating that fluid film volume was rapidly lost when scanning at lower humidity.

TABLE I. Mouse tibia sample and corresponding fluid film volume versus time gradient at 87% and 97%.

Sample	87% volumetric shrinkage rate (mm^3/min)	97% volumetric shrinkage rate (mm^3/min)
1	−0.0026	−0.0012
2	−0.0060	−0.0044
3	−0.0057	−0.0010
4	−0.0038	−0.0002
5	−0.0026	−0.0036
6	−0.0072	−0.0031
Mean ± SD	−0.0047 ± 0.0019	−0.0023 ± 0.0017

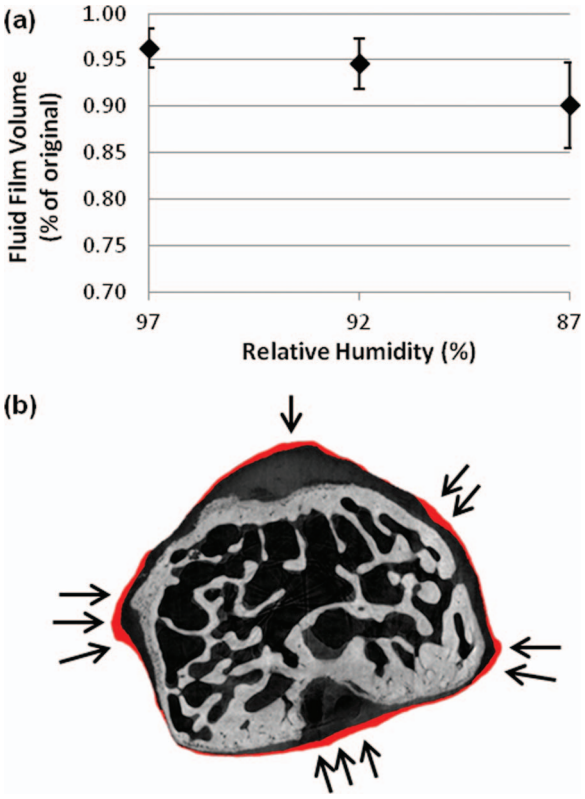

FIG. 6. (a) Fluid film volume percent after 24 min versus relative humidity for all six mice tibia. Loss of fluid film volume is evident at 87%. This is also shown in (b) the overlay of the μCT images at 87% and 92% relative humidity for a sample. The difference in fluid film thickness is shown by the red border as indicated by arrows.

A plot of fluid film volume normalized to original volume as a function of RH% is shown in Figure 6. When comparing the fluid film volume as percent of initial volume during the 16–24 min interval, the shrinkage due to dehydration was significantly larger when scanning at 87% compared to 97%. No significant difference was found between 87% and 92% or 92% and 97%. Additionally, no significant difference was found for any relative humidity level when comparing the fluid film volume during the 8–16 min interval. As such, a loss of fluid film volume was observed when scanning at decreasing levels of relative humidity, and this result was most pronounced between the 87% and 97% scans.

V. CONCLUSION AND DISCUSSION

The establishment of a quantitative measurement and analysis tool for the rapid and comprehensive evaluation of cartilage and bone in animal models is necessary for understanding arthritis and developing drugs for its treatment, as seen by the quantity of literature and methodologies tackling this challenge.[5,9,10,14,15,18,19] Recent imaging techniques such as EPIC-μCT have improved the visualization of cartilage with μCT scanning,[5–7] however, these methodologies can be hindered by the presence of motion artifact caused by tissue shrinkage when scanning at higher resolutions, see Figure 1.

This obstacle has been addressed in this paper with the development of a humidity chamber to assist with SR-μCT measurements. As the results of this validation study demonstrate, the humidity chamber can be used to obtain high-resolution, artifact-free μCT images in which cartilage and bone can be easily distinguished.

In this investigation, tissue dehydration and loss of fluid film volume over time was evident, especially over longer periods of time. This phenomenon could be represented as a volumetric shrinkage rate in mm^3/min. Samples scanned at progressively lower relative humidity levels were increasingly susceptible to tissue shrinkage over time. It was found that maintaining sample hydration throughout a scan was only possible at a RH% of 97% or higher. Therefore, with the help of the humidity chamber, cartilage samples can be scanned at 97% humidity to obtain SR-μCT images where the movement artifact caused by tissue dehydration is greatly reduced.

One of the difficulties encountered in this study was the ability to control and maintain low relative humidity levels. A discrepancy was observed in the actual relative humidity achieved when aiming for a level of 87%; measurements ranged from 87.3% to 95%. At a nominal humidity of 92%, the actual humidity ranged from 89.9% to 96.25%, while the relative humidity at 97% was more controllable, with actual humidity levels ranging from only 95.8% to 100.0%. This may have skewed some of the results, however, since it was shown that motion artifact could be effectively eliminated in scans from 97% relative humidity and above, which was a goal of this study, failure to maintain specific humidity levels below 92% is not considered a major drawback of the device.

The humidity chamber is currently custom-built for the TOMCAT beamline at the SLS. Since access to facilities for high-resolution SR-μCT is restricted, expensive, and highly limited, the development of a humidity chamber that is compatible with desktop μCT setups would be beneficial as it would allow for improved accessibility of this imaging technique to the rest of the scientific community. New design specifications would need to be defined for compatibility with desktop μCT, specifically space restrictions within the device. However, the increasingly high spatial resolution of recent systems makes such a device desirable. Furthermore, longitudinal studies of soft tissue engineering work would also be possible in a desktop μCT setup, as this has already been done for bone.[20]

Coupling this device with advances in synchrotron imaging such as phase contrast radiography[13] would allow the imaging of substructures (e.g., collagen fibres, cells) and their subsequent quantitative 3D morphometric analysis.[15,21,22] Furthermore, with the elimination of complications caused by sample manipulation, fixation, or destruction, the imaging of true 3D natural and whole joint structures can be realized.

The follow-on potential of this device used in conjunction with appropriate contrast agents for arthritis research is also very encouraging. Studies on preclinical animal models from small (e.g., mouse and rat on high-resolution systems) to large (rabbit and goat) would be enhanced by eliminating the need to fix the structures and cause unintended tissue damage. Additionally, imaging with the humidity chamber does not need to be limited to articular cartilage; any soft tissue or for that matter, any structure with a high water content (e.g., hydrogels and tissue-engineered constructs) would benefit from the technology.

In conclusion, the use of the humidity chamber during SR-μCT measurements was successfully validated. The results clearly show that loss of cartilage volume is associated with scanning at low humidity (87%). This effect can be avoided by using the humidity chamber to scan samples at 97% or above, since maintaining tissue hydration will reduce or eliminate cartilage shrinkage, and thus motion artifact.

ACKNOWLEDGMENTS

We thank Marco Hitz and Peter Schwilch for their technical support with the humidity chamber and nebulizer; Dr. Bernd Pinzer for beamtime support for the test experiments and providing technical support at the SLS; Thomas Steiner and Luc Nimeskern for their assistance with data collection and image processing; and Emma Cooling and Rachel Sondergaard for their valuable work on the early development of the humidity chamber.

This work was financially supported by the Swiss Commission for Technology and Innovation (CTI), Grant No. 9853.1.

[1] E. Darling, J. Hu, and K. Athanasiou, J. Orthop. Res. **22**, 1182 (2006).
[2] D. Gardner, Ann. Rheum. Dis. **31**, 235 (1972).
[3] B. Borah, E. Ritman, T. Dufresne, S. Jorgensen, S. Lui, J. Sacha, R. Phipps, and R. Turner, Bone **37**, 1 (2005).
[4] J. Moodie, K. Stok, R. Müller, T. Vincent, and S. Shefelbine, Osteoarthritis Cartilage **19**, 163 (2011).
[5] A. Palmer, R. Guldberg, and M. Levenston, Proc. Natl. Acad. Sci. U.S.A. **103**, 19255 (2006).
[6] L. Xie, A. Lin, R. Guldberg, and M. Levenston, Osteoarthritis Cartilage **18**, 65 (2010).
[7] P. Bansal, N. Joshi, V. Entezar, M. Grinstaff, and B. Snyder, Osteoarthritis Cartilage **18**, 184 (2010).
[8] J. Clark, J. Orthop. Res. **3**, 17 (1985).
[9] A. Thambyah, J. Zhao, S. Bevill, and N. Broom, J. Mech. Behav. Biomed. Mater. **5**, 206 (2012).
[10] K. Inagawa, T. Oohashi, K. Nishida, T. Tsubakishita, K. Yaykasli, A. Ohtsuka, T. Ozaki, T. Moriguchi, and Y. Ninomiya, Osteoarthritis Cartilage **17**, 1209 (2009).
[11] P. Suortti and W. Thomlinson, Phys. Med. Biol. **48**, R1 (2003).
[12] A. Thompson and J. Llacer, Nucl. Instrum. Methods **222**, 319 (1984).
[13] Y. Yarker, D. Hukins, and C. Nave, Connect. Tissue Res. **12**, 337 (1984).
[14] C. Choi, H. Kim, J. Choe, S. Kim, G. Choi, S. Jheon, and J. Kim, J. Synchrotron Radiat. **17**, 393 (2010).
[15] K. Stok and R. Müller, Microsc. Res. Tech. **72**, 650 (2009).
[16] F. Guilak, J. Microsc. **173**, 245 (1994).
[17] T. Hildebrand, A. Laib, R. Müller, J. Dequeker, and P. Rüegsegger, J. Bone Miner. Res. **14**, 1167 (1999).
[18] B. Wong, V. Wallace, M. Coleno, H. Benton, and B. Tromberg, Tissue Eng. **7**, 599 (2001).
[19] B. Fite, M. Decaris, Y. Sun, Y. Sun, A. Lam, C. Ho, J. Leach, and L. Marcu, Tissue. Eng. Part. C Methods **17**, 495 (2011).
[20] H. Hagenmüller, S. Hofmann, T. Kohler, H. Merkle, D. Kaplan, G. Vunjak-Novakovic, R. Müller, and L. Meinel, Ann. Biomed. Eng. **35**, 1657 (2007).
[21] D. Loessner, K. Stok, M. Lutolf, D. Hutmacher, J. Clements, and S. Rizzi, Biomaterials **31**, 8494 (2010).
[22] S. Voytik-Harbin, B. Roeder, J. Sturgis, K. Kokini, and J. Robinson, Microsc. Microanal. **9**, 74 (2003).